Available online at www.sciencedirect.com
ScienceDirect
Polymer 48 (2007) 1749–1755
polymer
www.elsevier.com/locate/polymer

Comparison of miscibility and structure of poly(3-hydroxybutyrate-*co*-3-hydroxyhexanoate)/poly(L-lactic acid) blends with those of poly(3-hydroxybutyrate)/poly(L-lactic acid) blends studied by wide angle X-ray diffraction, differential scanning calorimetry, and FTIR microspectroscopy

Tsuyoshi Furukawa [a,b], Harumi Sato [a], Rumi Murakami [a], Jianming Zhang [a,c], Isao Noda [d], Shukichi Ochiai [b], Yukihiro Ozaki [a,*]

[a] *School of Science and Technology and Research Center for Environment Friendly Polymers, Kwansei Gakuin University, 2-1 Gakuen, Sanda, Hyogo 669-1337, Japan*
[b] *S.T. Japan Inc., Minaminakaburi, Hirakata, Osaka 573-0094, Japan*
[c] *Department of Future Industry-oriented Basic Science and Materials, Graduate School of Engineering, Toyota Technological Institute, Hisakata, Tempaku, Nagoya 468-8511, Japan*
[d] *The Procter & Gamble Company, 8611 Beckett Road, West Chester, OH 45069, USA*

Received 21 September 2006; received in revised form 27 December 2006; accepted 12 January 2007
Available online 17 January 2007

Abstract

Comparison of miscibility and structure of poly((*R*)-3-hydroxybutyrate-*co*-(*R*)-3-hydroxyhexanoate) (P(HB-*co*-HHx)) ($M_w = 638{,}000$ g mol^{-1}) and poly(L-lactic acid) (PLLA) ($M_w = 150{,}000$ g mol^{-1}) with those of poly((*R*)-3-hydroxybutyrate) (PHB) ($M_w = 600{,}000$ g mol^{-1}), and PLLA having the blending ratios was investigated by wide angle X-ray diffraction (WAXD), differential scanning calorimetry (DSC), and infrared (IR) microspectroscopy techniques. WAXD reflection patterns show that the lattice parameters of *a* and *b* axes for PHB and P(HB-*co*-HHx) are unchanged in their blends with PLLA regardless of blending ratio. These WAXD results suggest that their crystalline structures are independent of the second component. The glass transition temperature (T_g) of blend components did not significantly change. The crystallization temperature (T_c) of PLLA reveal that both PHB/PLLA and P(HB-*co*-HHx)/PLLA blends form mixed semicrystalline systems. The T_c of PLLA in the PHB/PLLA blends and that in the P(HB-*co*-HHx)/PLLA blends shift to opposite directions indicating that both blends are immiscible but exhibit different levels of compatibilities. Micro IR spectra show that crystalline bands due to PHB appear even for the 20/80 blend but those due to PLLA are hardly observed for all the PHB/PLLA blends investigated. On the other hand, the crystalline bands of PLLA are observed in the micro IR spectra of some spots in the 20/80 P(HB-*co*-HHx)/PLLA blend. Micro IR spectra also show significant differences in the compatibility and crystalline structures between the P(HB-*co*-HHx)/PLLA and PHB/PLLA blends.

Keywords: Poly(3-hydroxybutyrate)/poly(L-lactic acid) blends; Poly(3-hydroxybutyrate-*co*-3-hydroxyhexanoate)/poly(L-lactic acid) blends; Crystalline structure

1. Introduction

Biodegradable polymers have been receiving keen interest as environmentally friendly materials. Poly(hydroxyalkanoates) (PHA)s are biosynthetic aliphatic polyesters produced and degraded by bacteria in soil [1–8]. Poly((*R*)-3-hydroxybutyrate) (PHB) is one of the most studied PHAs among biosynthetic polyesters. Some of the physical and mechanical properties of PHB are similar to those of petroleum-based polymers. However, PHB is rigid and stiff, and thus it is not always suitable for practical applications. One of the improvement methods for physical and mechanical properties of PHB is to blend

* Corresponding author. Tel.: +81 79 565 8349; fax: +81 79 565 9077.
E-mail address: ozaki@kwansei.ac.jp (Y. Ozaki).

0032-3861/$ - see front matter © 2007 Elsevier Ltd. All rights reserved.
doi:10.1016/j.polymer.2007.01.020

PHB with other polymers, including biodegradable polymers and conventional petroleum-based polymers [9–12]. Another effective improvement method is the copolymerization of PHB with other monomer units [13–16]. Poly((*R*)-3-hydroxybutyrate-*co*-(*R*)-3-hydroxyhexanoate) (P(HB-*co*-HHx)) is one of the promising PHA copolymers [1–4,8,14]. P(HB-*co*-HHx) has a lower crystallinity and higher flexibility than PHB and has good compatibility with other biodegradable and synthetic polymers. P(HB-*co*-HHx) shows biodegradability under both aerobic and anaerobic conditions. The physical and mechanical properties of P(HB-*co*-HHx) depend on the level of HHx comonomer content [1–4,8,14].

Poly(L-lactic acid) (PLLA) is a chemically synthesized aliphatic polyester and is also biodegradable [8,16–18]. One of the raw materials for PLLA is starch, which is harvested from corn, sweet potato, and so on. PLLA is synthesized via the ring-opening reaction of lactide that is prepared from fermentation products of starch. PLLA is degraded to lactic acid that already exists in human body. Therefore, PLLA has good biocompatibility and has already been used in many applications. One of the most popular applications of PLLA lies in the medical field; PLLA is used as a drug delivery system (DDS) [19,20], implants [21], and bone fixation [22]. In some applications, PLLA is superior to other biodegradable polyesters, because of the better thermal and mechanical properties, as well as the excellent transparency of products.

PHB and PLLA have been blended with various biodegradable and nonbiodegradable polymers for the improvement of their physical and mechanical properties [9,11,23–27]. The morphology, thermal behavior, miscibility, and physical properties of different kinds of PHB blends and PLLA blends have been investigated. Poly(ethylene glycol) (PEG) is one of the most widely used materials blended with PHB [9] or PLLA [23–27]. The thermal behavior and miscibility of their blends depend on the molecular weight of PEG.

The miscibility and crystallinity of PHB/PLLA blends have also been investigated [28–34]. The molecular weight of PHB influences the miscibility of PHB/PLLA blends; only PHB with a low molecular weight is fully miscible with PLLA [28,29]. On the other hand, PHB is miscible with low molecular weight PLLA in the melt over the whole composition range [30,31]. The crystallinity and growth rate of spherulitic structure of PHB are affected by the blending ratio of PHB/PLLA blends [33,34].

Several research groups have already reported the physical and mechanical properties of the P(HB-*co*-HHx)/PLLA blends [35] and the possible existence of different crystalline forms of P(HB-*co*-HHx) [36]. Noda et al. investigated the physical and mechanical properties, energy-to-break toughness, and transparency of P(HB-*co*-HHx) (HHx = 5 mol%)/PLLA blends with different blending ratios [35]. They also analyzed the state of crystallization of these blends by using temperature-dependent IR spectra [35]. Marcott et al. studied P(HB-*co*-HHx)/PLLA blends with different blending ratios by combining temperature-dependent IR spectra with chemometrics and two-dimensional correlation analysis [36]. They revealed the early disappearance of more-ordered crystalline P(HB-*co*-HHx) on heating the sample and the formation of the amorphous P(HB-*co*-HHx) before the complete disappearance of less-ordered crystalline P(HB-*co*-HHx). These studies, based mainly on the analysis of C=O stretching bands, suggested that the crystallization of P(HB-*co*-HHx) and PLLA in the blends depends on the domain sizes of each component [36].

IR spectroscopy enables one to explore the structure and interaction of molecules at the functional group level. For this reason, IR spectroscopy has extensively been used to elucidate the crystalline and amorphous structure of polymers [34–43]. Microspectroscopy is a very powerful tool of microanalysis for very small samples or small regions within a larger sample to extract chemical information about materials. It has micrometer order spatial resolution, so that it is possible to investigate the microstructure of inhomogeneous blends as well as that of homogeneous samples.

We have investigated the structure and thermal behavior of PHB and three kinds of P(HB-*co*-HHx) with different HHx contents by using IR spectroscopy and wide angle X-ray diffraction (WAXD) [41,42]. We found the existence of an intermolecular C–H···O=C hydrogen bond between the C=O group and the CH_3 group in PHB and P(HB-*co*-HHx). The CH stretching band at 3009 cm^{-1} due to the C–H···O=C hydrogen bond shifts gradually to a lower wavenumber with temperature in the temperature-dependent IR spectra from just above room temperature [37]. This observation indicates that the weakening of the C–H···O=C hydrogen bond proceeds gradually even from fairly low temperature. Our other studies have shown the differences in C–H···O=C interactions among PHB, PLLA, and PLLA/poly(D-lactide)(PLLA/PDLA) stereocomplex [43]. In the case of PHB, there are a chain of C–H···O=C hydrogen bond pairs that combine two parallel helical structures, stabilizing the chain folding of PHB crystalline units. In the PLLA/PDLA stereocomplex system, the C–H···O=C interaction may be ascribed to the intermolecular hydrogen bond. As for PLLA, there is no strong hydrogen bond among the PLLA chains, and only dipole–dipole interactions and van der Waals interactions are involved.

Structure, dispersibility, and crystallinity of PHB/PLLA blends with the blending ratios of 80/20, 60/40, 40/60, and 20/80 were investigated by polarized light microscopy, micro IR spectroscopy, and differential scanning calorimetry (DSC) in our previous study [34]. In that study the spherulitic structure of PHB was not observed in the 20/80 blend by means of polarized light microscopy and micro IR spectra. IR bands arising from nonspherulitic parts were observed for both PHB and PLLA in all the blends investigated. In the DSC curves, the temperatures of melt and crystallization of PHB and PLLA were almost the same for all the blends. These results suggested that the PHB/PLLA blends are immiscible and inhomogeneous system.

In the present study, four kinds of PHB/PLLA and P(HB-*co*-HHx) (HHx = 12 mol%)/PLLA blends with the PLLA content ranging from 20 to 80 wt% have been investigated by using WAXD, DSC and IR microspectroscopy to elucidate the miscibility, structure, and crystallinity of P(HB-*co*-HHx)/

PLLA blends. The results of both blend systems are then compared with each other. This study revealed the difference of the miscibility of PHB/PLLA and P(HB-*co*-HHx)/PLLA blends.

2. Experimental part

2.1. Preparation of blends

The chemical structures of PHB, P(HB-*co*-HHx), and PLLA are shown in Fig. 1. PHB ($M_w = 600{,}000\ g\ mol^{-1}$, $M_w/M_n = 2.2$) and P(HB-*co*-HHx) ($M_w = 638{,}000\ g\ mol^{-1}$, $M_w/M_n = 2.4$) were obtained from the Procter & Gamble Company and PLLA ($M_w = 150{,}000\ g\ mol^{-1}$, $M_w/M_n = 1.8$) was obtained from Shimadzu Corporation (LACTY5000). The composition of HHx in P(HB-*co*-HHx) was 12 mol%. Since P(HB-*co*-HHx) is a random copolymer, P(HB-*co*-HHx) means that the probability of finding two consecutive units of 3HB is ca. 0.9[2]. Blends of PHB and PLLA and those of P(HB-*co*-HHx) and PLLA were prepared by dissolving each component together in hot chloroform, and then the solution was cast on a aluminum dish as a film. The blending ratios of PHB/PLLA blends and P(HB-*co*-HHx)/PLLA blends were 80/20, 60/40, 40/60, and 20/80 by weight.

2.2. Wide angle X-ray diffraction (WAXD)

WAXD data for PHB/PLLA blends and P(HB-*co*-HHx)/PLLA blends were measured at room temperature in the scattering angle range of $2\theta = 2–40°$ by using RIGAKU RINT 2000. Cu Kα radiation (wavelength, 1.5418 nm) from an X-ray generator was used as an incident X-ray source (40 kV, 20 mA).

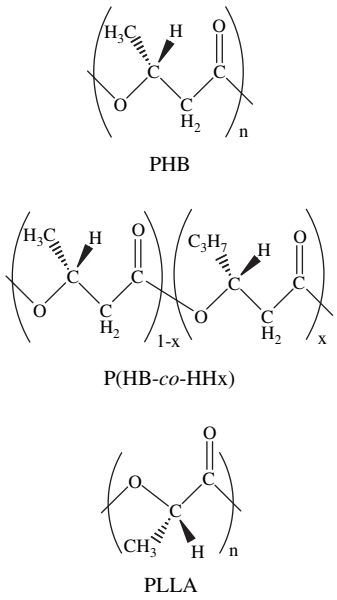

Fig. 1. Chemical structures of PHB, P(HB-*co*-HHx), and PLLA.

2.3. Differential scanning calorimetry (DSC)

DSC measurements were performed on a Perkin–Elmer Pyris6 DSC system over a temperature range from −10 to 190 °C at heating and cooling rates of 20 °C min^{-1}. The analysis of DSC curves was carried out for the second heating run data. The sample films (5–6 mg) were sealed in aluminum pans.

2.4. FTIR microspectroscopy

IR spectra were measured at a 4 cm^{-1} spectral resolution with a FTIR microspectrometer (IlluminatIR, Smith Detection) equipped with a mercury cadmium telluride (MCT) detector, and 512 scans were co-added. Micro IR spectra were collected at a 4 cm^{-1} spectral resolution by attenuated total reflection (ATR) mode. The ATR element used was made of type II diamond (refractive index is 2.42) with the incident angle of 45°. The spatial resolution was 12 μm diameter.

3. Results and discussion

3.1. WAXD

The WAXD patterns of PHB/PLLA blends and P(HB-*co*-HHx)/PLLA blends are shown in Fig. 2A and B. The crystalline structure of PHB has been well established to be orthorhombic with lattice parameters of $a = 5.72$ Å and $b = 13.12$ Å with its chain conformation in the left-handed 2_1 helix [44,45]. On the other hand, as for the crystalline structure (α form) of PLLA, there are two main opinions on the chain conformation of PLLA in the unit cell. One is the "pure" 10_3 helix regular [47,48], and the other is the so-called "distorted" 10_3 helix conformation owing to the interchain interactions between CH_3 groups [46]. In the WAXD patterns of neat PHB and P(HB-*co*-HHx), the (020) and (110) reflection peaks are observed, respectively, at 13.5° and 16.9°. In the case of PLLA, the WAXD pattern shows the (010) reflection peak at 14.8°, and the (110) and (200) reflection peaks at 16.7°.

As can be seen in Fig. 2A and B, although the reflection peaks of PHB are observed even for the 20/80 PHB/PLLA blend, those of P(HB-*co*-HHx) are not identified for the 20/80 P(HB-*co*-HHx)/PLLA blend. Since the crystallinity and the crystal growth rate of PHB are higher and faster than those of P(HB-*co*-HHx) the reflection peaks of PHB are observed even in the blends with higher PLLA content. On the other hand, PLLA reflection peaks are found only in the PLLA-rich blends for both the blends with PHB and P(HB-*co*-HHx). The *a* and *b* lattice parameters of each component in PHB/PLLA and P(HB-*co*-HHx)/PLLA blends are summarized in Table 1. The lattice parameters are almost unchanged in PHB/PLLA and P(HB-*co*-HHx)/PLLA blends irrespective of the blending ratios. This result suggests that each component in the blends forms its crystalline structure independently of the second component [32]. The WAXD results also revealed that both PHB/PLLA and P(HB-*co*-HHx)/PLLA blends are immiscible.

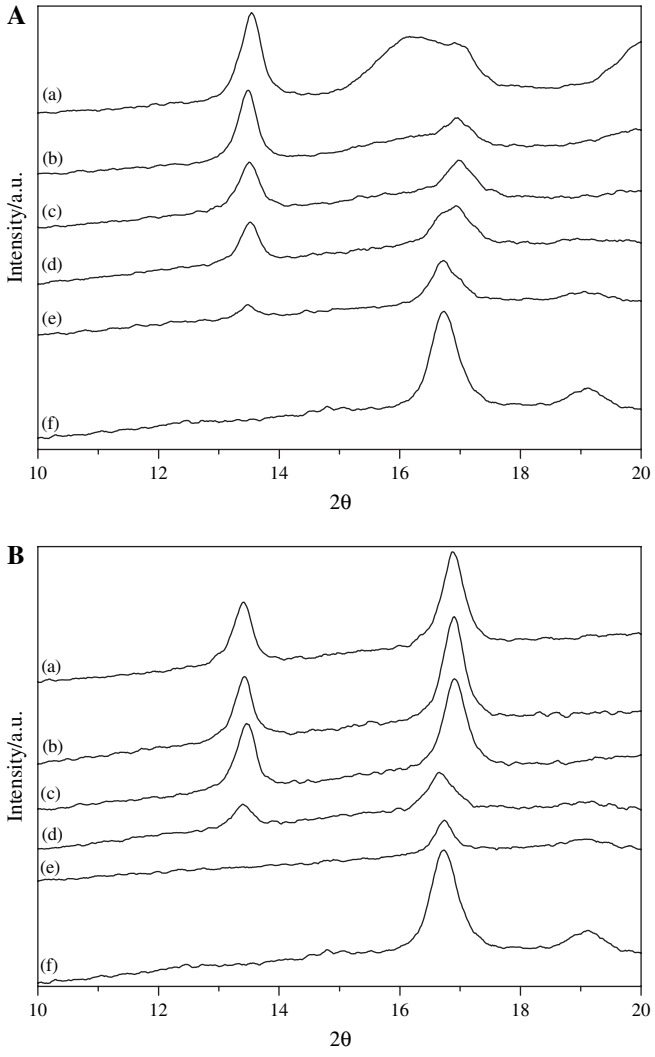

Fig. 2. WAXD patterns of (A) PHB/PLLA and (B) P(HB-*co*-HHx)/PLLA blends. (a) PHB (P(HB-*co*-HHx)), (b) 80/20 blend, (c) 60/40 blend, (d) 40/60 blend, (e) 20/80 blend and (f) PLLA.

3.2. DSC

Fig. 3A and B displays the second heating processes observed in the DSC scans during the heating of PHB/PLLA blends and P(HB-*co*-HHx)/PLLA blends from −10 to 190 °C. The glass transition temperature (T_g), the crystallization temperature (T_c) and the melting temperature (T_m) of all samples are listed in Table 2. The T_g of neat PHB, P(HB-*co*-HHx), and PLLA are 4.0, 2.8, and 61.6 °C, respectively. The T_g of PHB and PLLA in their blends are 4.0−6.9 and 57.0−61.8 °C, respectively. Those of P(HB-*co*-HHx) and PLLA in their blends are 3.7−4.7 and 64.8−67.8 °C, respectively. However, it is difficult to detect the T_g value of P(HB-*co*-HHx) in the 20/80 blend because of the low P(HB-*co*-HHx) content. The DSC curves of PHB/PLLA (P(HB-*co*-HHx)/PLLA) blends exhibit two T_g values of PHB (P(HB-*co*-HHx)) and PLLA, and the differences of them in the blends do not show remarkable changes. This observation indicates that both blend systems are immiscible systems [31,32]. The peak positions of the detected T_g are indicated by the arrows in Fig. 3A and B.

Although the T_c of neat PLLA appears at 122.8 °C, those of PHB and P(HB-*co*-HHx) cannot be detected. The T_c of PLLA is observed also in both blend systems except for the 20/80 P(HB-*co*-HHx)/PLLA blend. This result suggests that both PHB/PLLA and P(HB-*co*-HHx)/PLLA blends are mixed semicrystalline systems. Since both PHB/PLLA and P(HB-*co*-HHx)/PLLA blends are immiscible, the crystals of both components exist side by side. In the PHB/PLLA blends, the T_c peak appears in the temperature range of 109.4−130.3 °C and is influenced by the blending ratio. The T_c peak shifts to lower temperature with the increase in the PHB contents. This result suggests that a small amount of PLLA component disperses in the PHB phase [31]. In the P(HB-*co*-HHx)/PLLA blends, although the T_c value of PLLA for the blends shifts slightly to high temperature in comparison with neat PLLA, there is no clear relationship between the T_c values and the blending ratio. For the miscible blends of PHB and PLLA with low molecular weight, the increase in T_c suggests that the crystallization process takes place from a single homogeneous phase [31]. Therefore, the increase of T_c value with increasing PLLA component leads us to conclude that P(HB-*co*-HHx)/PLLA blends are immiscible but have higher compatibility than PHB/PLLA blends. The peak positions of the T_c of PLLA are also indicated by the arrows in Fig. 3A and B.

Table 1
The *a* and *b* lattice parameters of PHB, P(HB-*co*-HHx), and PLLA

	PHB, P(HB-*co*-HHx)		PLLA	
	a lattice parameter/Å	*b* lattice parameter/Å	*a* lattice parameter/Å	*b* lattice parameter/Å
PHB	5.72	13.12	–	–
80/20 PHB/PLLA	5.72	13.12	n.d.	n.d.
60/40 PHB/PLLA	5.68	13.12	n.d.	n.d.
40/60 PHB/PLLA	5.72	13.12	10.62	n.d.
20/80 PHB/PLLA	n.d.	13.12	10.62	n.d.
P(HB-*co*-HHx)	5.72	13.21	–	–
80/20 P(HB-*co*-HHx)/PLLA	5.72	13.19	n.d.	n.d.
60/40 P(HB-*co*-HHx)/PLLA	5.72	13.18	n.d.	n.d.
40/60 P(HB-*co*-HHx)/PLLA	n.d.	13.22	10.62	n.d.
20/80 P(HB-*co*-HHx)/PLLA	n.d.	n.d.	10.59	n.d.
PLLA	–	–	10.60	5.99

n.d.: not detected.

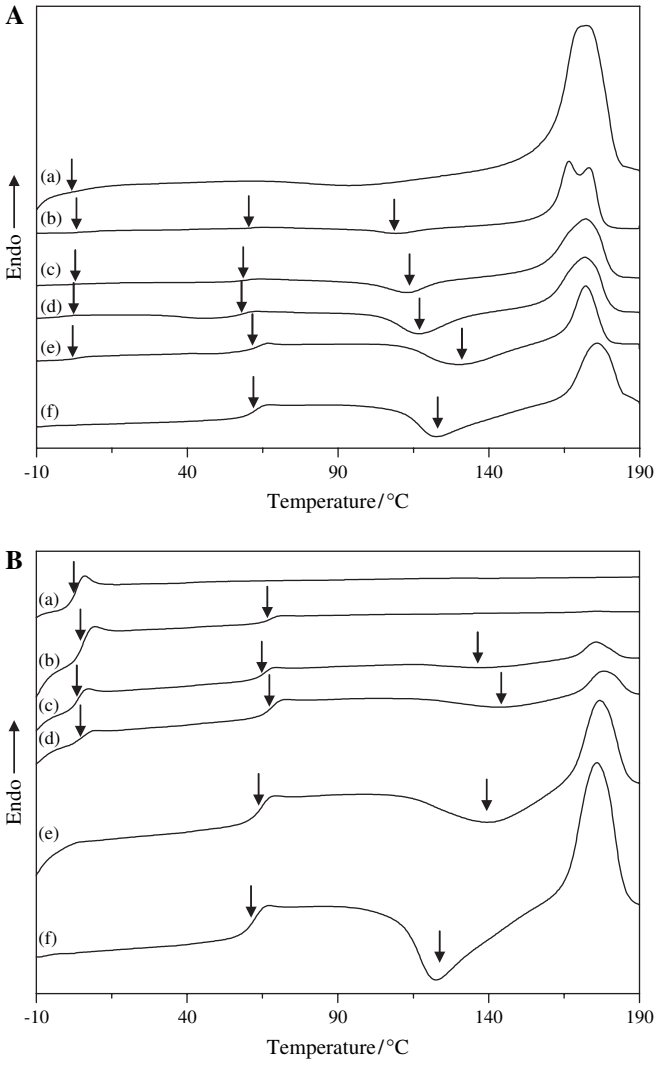

Fig. 3. DSC scans during the heating processes of (A) PHB/PLLA and (B) P(HB-*co*-HHx)/PLLA blends from −10 to 190 °C. (a) PHB (P(HB-*co*-HHx)), (b) 80/20 blend, (c) 60/40 blend, (d) 40/60 blend, (e) 20/80 blend, and (f) PLLA. The peak positions of T_g and T_c for the blend components are indicated by the arrows.

Table 2
Thermal properties of the PHB/PLLA and P(HB-*co*-HHx)/PLLA blends

	T_g/°C			T_c/°C	T_m/°C
	PHB	P(HB-*co*-HHx)	PLLA	PLLA	
PHB	4.0	–	–	–	168.4 175.0
80/20 PHB/PLLA	6.9	–	61.0	109.4	166.3 174.3
60/40 PHB/PLLA	6.7	–	58.7	112.5	172.1
40/60 PHB/PLLA	5.1	–	57.0	116.8	171.8
20/80 PHB/PLLA	4.0	–	61.8	130.3	172.0
P(HB-*co*-HHx)	–	2.8	–	–	120.4
80/20 P(HB-*co*-HHx)/PLLA	–	4.7	66.8	n.d.	175.7
60/40 P(HB-*co*-HHx)/PLLA	–	3.7	64.9	137.4	175.3
40/60 P(HB-*co*-HHx)/PLLA	–	4.7	67.8	143.4	178.1
20/80 P(HB-*co*-HHx)/PLLA	–	n.d.	64.8	139.6	176.7
PLLA		–	61.6	122.8	176.1

n.d.: not detected.

The T_m peaks of neat PHB are observed at 168.4 and 175.0 °C as double peaks. Yoshie et al. and Abe et al. reported that the lower and higher peaks are assigned, respectively, to the melting peak of crystals formed at T_c and the melting peak of crystals which are recrystallized during the heating process [13,14]. The T_m of PLLA at 176.1 °C is overlapped with those of PHB in the PHB/PLLA blends. Therefore, it is difficult to identify each T_m peak in the PHB/PLLA blends. Although the T_m peak of P(HB-*co*-HHx) is very weak because of its low crystallinity, it appears at 120.4 °C. However, this temperature is close to the T_c of PLLA, and the intensity of the T_c of PLLA is stronger than that of T_m peak of P(HB-*co*-HHx). Therefore, in the P(HB-*co*-HHx)/PLLA blends, only the T_c of PLLA can be identified.

3.3. FTIR microspectroscopy

Fig. 4A and B shows micro IR spectra in the 2000–1000 cm^{-1} region of PHB/PLLA and P(HB-*co*-HHx)/PLLA

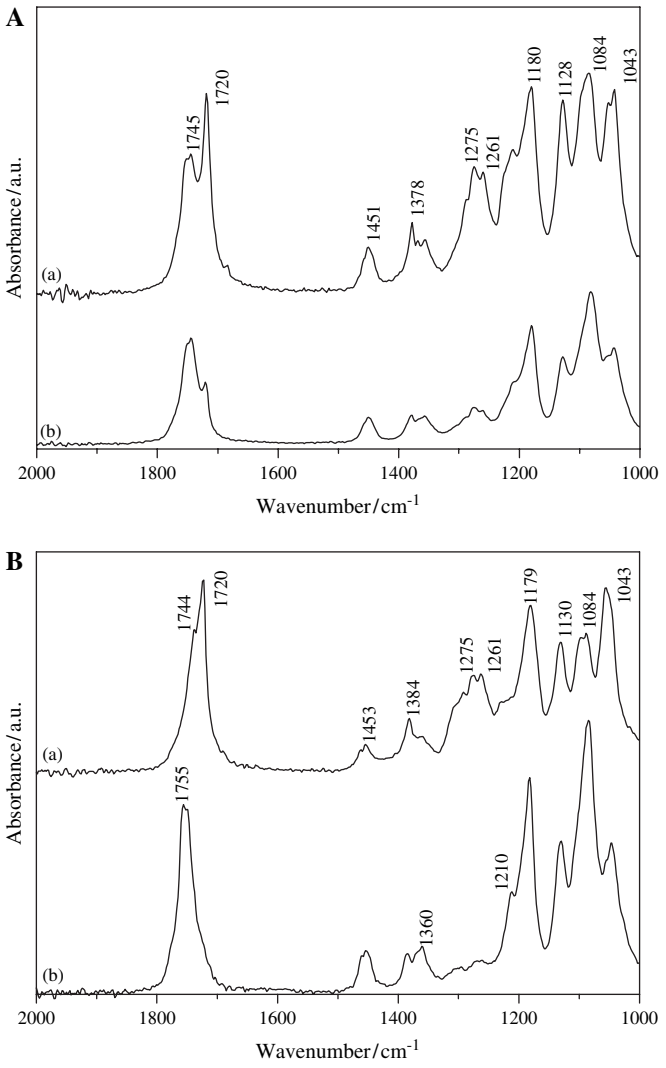

Fig. 4. Micro IR spectra of (A) PHB/PLLA and (B) P(HB-*co*-HHx)/PLLA blends. (a) 80/20 blend and (b) 20/80 blend.

Table 3
Wavenumbers (cm^{-1}) and assignments of IR bands of PHB, P(HB-*co*-HHx), and PLLA

	PHB, P(HB-*co*-HHx)	PLLA
1755		C=O stretching (C)
1744		C=O stretching (A)
1720	C=O stretching (C)	
1453	CH_3 asymmetric deformation	CH_3 asymmetric deformation
1384	CH_3 symmetric deformation	CH_3 symmetric deformation
1356	CH deformation and CH_3 symmetric deformation	CH deformation and CH_3 symmetric deformation (C)
1275	C–O–C stretching (C)	
1265		C–O–C stretching + CH deformation (A)
1261	C–O–C stretching + CH deformation (C)	
1210		C–O–C stretching (C)
1179	C–O–C stretching	C–O–C stretching
1130	CH_3 rocking	
1084		C–O–C stretching
1043	C–CH_3 stretching	C–CH_3 stretching

A: amorphous, C: crystalline.

blends with the 80/20 and 20/80 blending ratio. The differences in the IR spectra between neat PHB and P(HB-*co*-HHx) lie mainly in the intensities of crystalline and amorphous bands [37,38,42]. Assignments of IR bands of PHB, P(HB-*co*-HHx), and PLLA are summarized in Table 3. In our previous micro IR study of PHB/PLLA blends, crystalline bands of PHB were clearly observed, but those of PLLA were not identified in the micro IR spectra of the 80/20 and 20/80 blends [34]. The ratios of peak intensities of PHB and PLLA bands are dependent on measurement points in both blends. In the 80/20 PHB/PLLA blend, the spectra of many spots are similar to the crystalline PHB spectrum. The observed main PHB crystalline bands are as follows: the C=O stretching band at 1720 cm^{-1}, C–O–C stretching band at 1275 cm^{-1}, and the band at 1261 cm^{-1} due to the coupling of C–O–C stretching and CH deformation modes. These bands are clearly identified in the spectra shown in Fig. 4A(a) and B(a). The spectra including amorphous PLLA bands at 1745 cm^{-1} are obtained in some spots as shown in Fig. 4A(a). As can be seen in Fig. 4A(b), the crystalline C=O stretching band at 1720 cm^{-1} due to PHB is observed anywhere in the 20/80 PHB/PLLA blend. The crystalline C=O stretching band of PLLA at 1755 cm^{-1} appears weak also for any spots. Other PLLA crystalline bands at 1356 and 1210 cm^{-1} assigned, respectively, to the coupling of CH deformation and CH_3 symmetric deformation mode and the C–O–C stretching mode are also not so strong. These results indicate that the crystallization of PHB is relatively easy and that of PLLA components is hard, even in the 20/80 PHB/PLLA blend [34].

In the case of P(HB-*co*-HHx)/PLLA blends, the intensity ratios of P(HB-*co*-HHx) and PLLA bands are also dependent on measurement points of locations in the 80/20 and 20/80 blends. In the 80/20 P(HB-*co*-HHx)/PLLA blend, the crystalline bands of P(HB-*co*-HHx) are also observed, but those of PLLA are absent in the spectra from any spots as shown in Fig. 4B(a). The weak amorphous bands of PLLA are observed in the spectra of 80/20 P(HB-*co*-HHx)/PLLA blend. On the other hand, the crystalline and amorphous bands of P(HB-*co*-HHx) are not observed in the spectra of some spots of the 20/80 P(HB-*co*-HHx)/PLLA blend (Fig. 4B(b)). One of the most characteristic amorphous bands of PLLA at 1265 cm^{-1} assigned to the coupling of C–O–C stretching and CH deformation modes is also missing in the spectra of the 20/80 P(HB-*co*-HHx)/PLLA blend. Thus, the spectra from some spots of the 20/80 P(HB-*co*-HHx)/PLLA blend are very similar to the neat crystalline PLLA spectra.

These results for IR microspectroscopy reveal that PHB and P(HB-*co*-HHx) are crystallized but not PLLA in the 80/20 blends. These are in good agreement with the WAXD results that the reflection peaks of only PHB and P(HB-*co*-HHx) are observed in the 80/20 blends. Moreover, the observation of the existence of PHB crystalline bands, contrasting the absence of the P(HB-*co*-HHx) crystalline bands in the spectra of the 20/80 blends are also in good agreement with WAXD results that the reflection peaks are observed only for PHB and not for P(HB-*co*-HH). These results also indicate that P(HB-*co*-HHx) component dispersed in a PLLA matrix at a relatively low level does not crystallize much [35].

4. Conclusion

In this study, the miscibility and structure of PHB/PLLA and P(HB-*co*-HHx)/PLLA blends are investigated by using DSC, WAXD, and IR microspectroscopy. The results are then compared between the two kinds of blends. The following conclusions can be reached from the present study.

The combination of DSC, WAXD, and IR microspectroscopy revealed that both PHB/PLLA and P(HB-*co*-HHx)/PLLA blends are immiscible, but the P(HB-*co*-HHx)/PLLA blends are somewhat more compatible.

WAXD reflection patterns revealed that PHB component can be crystallized in the PHB/PLLA blends with any ratio and that P(HB-*co*-HHx) component can also be crystallized in the P(HB-*co*-HHx)/PLLA blends except for the 20/80 blend. The *a* and *b* lattice parameters of each component in the blends are almost constant, suggesting that their crystalline structures are kept intact in the blends.

The T_g values for P(HB-*co*-HHx) and PLLA components in the P(HB-*co*-HHx)/PLLA blends also do not change significantly, as well as the case of those for PHB and PLLA component in the PHB/PLLA blends. The observation of the T_c of PLLA in both blend systems suggests that each component in not only the PHB/PLLA but also P(HB-*co*-HHx)/PLLA blends forms the mixed semicrystalline structures. The T_c of PLLA in the PHB/PLLA and P(HB-*co*-HHx)/PLLA blends shift, respectively, to lower and higher temperature with the increase in the PHB or P(HB-*co*-HHx) component. These results indicate that the PHB/PLLA blends with decreasing T_c are totally immiscible, while the P(HB-*co*-HHx)/PLLA blends with increasing T_c are somewhat compatible.

Micro IR spectra from any spots of the 80/20 PHB/PLLA and P(HB-*co*-HHx)/PLLA blends show the crystalline bands only due to PHB and P(HB-*co*-HHx) components but not for PLLA. On the other hand, although the micro IR spectra from any spots of the 20/80 PHB/PLLA blend also show the crystalline bands due to PHB, those from some spots of the 20/80 P(HB-*co*-HHx)/PLLA blend show only the crystalline bands of PLLA component. P(HB-*co*-HHx) dispersed in a PLLA matrix at this low level does not crystallize.

Acknowledgements

This work was partially supported by ''Open Research Center'' project for private universities: matching fund subsidy from MEXT (Ministry if Education, Culture, Sports, Science and Technology), 2001–2005. This work was also supported by Kwansei Gakuin University ''Special Research'' project, 2004–2008.

References

[1] Doi Y, Steinbuchel A, editors. Biopolymers. Polyesters I–III, vols. 3a, 3b and 4. Weinheim: Wiley-VCH; 2001.
[2] Doi Y. Microbial polyesters. New York: VCH Publishers; 1990.
[3] Satkowski MM, Melik DH, Autran JP, Green PR, Noda I, Schechtman LA. In: Steinbüchel A, Doi Y, editors. Biopolymers. Weinheim: Wiley-VCH; 2001. p. 231.
[4] Doi Y, Kitamura S, Abe H. Macromolecules 1995;28(14):4822–8.
[5] Anderson AJ, Dawes EA. Microbiol Rev 1990;54:450–72.
[6] Dawes EA. Novel biodegradable microbial polymers. Dordrecht: Kluwer; 1990.
[7] Lara LM, Gjalt WH. Microbiol Mol Biol Rev 1991;63(1):21–53.
[8] Iwata T, Doi Y. Macromol Chem Phys 1999;200(11):2429–42.
[9] Avella M, Martuscelli E. Polymer 1988;29(10):1731–7.
[10] Greco P, Martuscelli E. Polymer 1989;30(8):1475–83.
[11] Azuma Y, Yoshie N, Sakurai M, Inoue Y, Chujo R. Polymer 1992;33(22): 4763–7.
[12] Gassner F, Owen AJ. Polymer 1994;35(10):2233–6.
[13] Yoshie N, Menju H, Sato H, Inoue Y. Macromolecules 1995;28(19): 6516–21.
[14] Abe H, Doi Y, Aoki H, Akehata T. Macromolecules 1998;31(6):1791–7.
[15] Yoshie N, Saito M, Inoue Y. Macromolecules 2001;34(26):8953–60.
[16] Dorgan JR. Poly(lactic acid), properties and prospects of an environmentally benign plastic. Washington, DC: American Chemical Society; 1999. p. 145–9.
[17] Ikada Y, Tsuji H. Macromol Rapid Commun 2000;21(3):117–32.
[18] Urayama H, Kanamori T, Kimura Y. Macromol Mater Eng 2002;287(2): 116–21.
[19] Schakenraad JM, Oosterbaan JA, Nieuwenhuis P, Molenaar I, Olijslager J, Potman W, et al. Biomaterials 1988;9(1):116–20.
[20] Jackanicz TM, Nash HA, Wise DL, Gregory JB. Contraception 1973; 8(3):227–34.
[21] Penning JP, Dijkstra H, Pennings AJ. Polymer 1993;34(5):942–51.
[22] Leenslag JW, Pennings AJ, Bos RRM, Rozema FR, Boering G. Biomaterials 1987;8(4):311–4.
[23] Nakafuku C. Polym J 1996;28(7):568–75.
[24] Younes H, Cohn D. Eur Polym J 1988;24(8):765–73.
[25] Hu Y, Hu YS, Topolkaraev V, Hiltner A, Baer E. Polymer 2003;44(19): 5681–9.
[26] Hu Y, Rogunova M, Topolkaraev V, Hiltner A, Baer E. Polymer 2003; 44(19):5701–10.
[27] Hu Y, Hu YS, Topolkaraev V, Hiltner A, Baer E. Polymer 2003;44(19): 5711–20.
[28] Gazzano M, Focarete ML, Riekel C, Scandola M. Biomacromolecules 2004;5(2):553–8.
[29] Ohkoshi I, Abe H, Doi Y. Polymer 2000;41(15):5985–92.
[30] Blümm E, Owen AJ. Polymer 1995;36(21):4077–81.
[31] Koyama N, Doi Y. Polymer 1997;38(7):1589–93.
[32] Park JW, Doi Y, Iwata T. Biomacromolecules 2004;5(4):1557–66.
[33] Zhang L, Xiong C, Deng X. Polymer 1996;37(2):235–41.
[34] Furukawa T, Sato H, Murakami R, Zhang J, Duan YX, Noda I, et al. Macromolecules 2005;38(15):6445–54.
[35] Noda I, Satkowski MM, Dowery AE, Marcott C. Macromol Biosci 2004; 4(3):269–75.
[36] Marcott C, Dowrey AE, Poppel JV, Noda I. Vib Spectrosc 2004;36(2): 221–5.
[37] Sato H, Murakami R, Padermshoke A, Hirose F, Senda K, Noda I, et al. Macromolecules 2004;37(19):7203–13.
[38] Sato H, Dybal J, Murakami R, Noda I, Ozaki Y. J Mol Struct 2005; 744–747:35–46.
[39] Zhang J, Tsuji H, Noda I, Ozaki Y. Macromolecules 2004;37(17): 6433–9.
[40] Zhang J, Tsuji H, Noda I, Ozaki Y. J Phys Chem B 2004;108(31): 11514–20.
[41] Sato H, Nakamura M, Padermshoke A, Yamaguchi H, Terauchi H, Ekgasit S, et al. Macromolecules 2004;37(10):3763–9.
[42] Sato H, Padermshoke A, Nakamura M, Murakami R, Hirose F, Senda K, et al. Macromol Symp 2005;220(1):123–38.
[43] Zhang J, Sato H, Tsuji H, Noda I, Ozaki Y. J Mol Struct 2005;735–736: 249–57.
[44] Yokouchi M, Chatani Y, Tadokoro H, Teranishi K, Tani H. Polymer 1973;14(6):267–72.
[45] Okamura K, Marchessault RH. In: Ramachandran GN, editor. Conformation of biopolymers, vol. 2. New York: Academic Press; 1967. p. 709.
[46] Hoogsteen W, Postema AR, Pennings AJ, ten Brinke G, Zugenmaier P. Macromolecules 1990;23(2):634–42.
[47] De Santis P, Kovacs AJ. Biopolymers 1968;6(3):299–306.
[48] Kobayashi J, Asahi T, Ichiki M, Okikawa A, Suzuki H, Watanabe T, et al. J Appl Phys 1995;77(7):2957–73.